

# Infrared Spectroscopic studies on the Mobility of Metamorphic Fluid in Quartz veins of Dharwar Craton

D. Srinivasa Sarma, M. Ram Mohan and P.S.R. Prasad\*

National Geophysical Research Institute, (Council of Scientific & Industrial Research), HYDERABAD – 500 606 (India)

**Abstract:** The thermal induced variations of water inclusions in their OH stretching mode region were probed in quartz veins from Dharwar Craton, India, using fourier transformed infrared spectroscopy (FTIR) in the temperature range 25 to 300 °C. All the inclusions have composition H<sub>2</sub>O-NaCl-CO<sub>2</sub>. The peak positions monotonously shift to higher wavenumbers with increasing temperature with slopes of 0.23 and 0.43 cm<sup>-1</sup> °C<sup>-1</sup> for the inclusions of Eastern and Western Dharwar Craton, respectively. The effect of CO<sub>2</sub> on the mobility of water inclusions was also investigated and our results indicate higher mobility for CO<sub>2</sub> rich inclusions.

**Keywords:** Metamorphic fluids, dharwar craton, quartz veins, FTIR spectroscopy.

## INTRODUCTION

Fluids like carbon dioxide and water are ubiquitous in most of the metamorphic and volcanic rocks. These fluids are highly mobile and are important in several metamorphic processes [1]. Mobility of these fluids is controlled by the pore geometry and related permeability of rock-fluid interactions in general and metamorphic rocks in particular [2-5].

In diagenetic or metamorphic rocks recrystallized under static conditions, the geometry of the fluid-filled equilibrated pores is controlled by the dihedral (wetting) angle ( $\theta$ ), which depends on temperature, pressure, mineralogy of host matrix and composition of the fluid phase [6-8]. Theoretical models predict that if  $\theta < 60^\circ$ , the grain edge channels remain open, thus enabling the fluid phase to form a stable interconnected network along which fluid flow can occur. Conversely, if  $\theta > 60^\circ$  the pores get closed and the fluid will get collected at grain corners making the rock impermeable. In other words, the fluid phase can form a stable interconnected network of grain-edge channels along which flow can occur only if the dihedral angle is below  $60^\circ$ . If the dihedral angle exceeds this critical value then the fluids exist in isolated pores within the solid matrix, which is then impermeable to grain-edge flow. Normally, the fluids entrapped in minerals like quartz were alleged as “closed”, preserving information on their genetic evolution. However, in the recent five to six years there has been a host of experimental and theoretical evidences against the closeness of fluid inclusions, which are suggested to migrate into or out of the host mineral or rock under favorable conditions [3, 4].

Holness reported detailed investigations on the equilibrium dihedral angle in the quartz-CO<sub>2</sub>-H<sub>2</sub>O-NaCl system and observed that it significantly depends on composition, pressure and temperature [7]. The dihedral angle in quartz-H<sub>2</sub>O was reported as  $77^\circ$  at around 1.5 kbar and that salinity decreases it close to its critical value ( $60^\circ$ ), while addition of CO<sub>2</sub> increases to the angle to  $95^\circ$ . However, measurement of permeability using dihedral angles in natural rock formations is often associated with large errors as the resultant pore geometry is highly influenced by several deformational and metamorphic processes. Additionally, structural properties of H<sub>2</sub>O significantly vary by the addition of NaCl and CO<sub>2</sub>. Carbon dioxide and H<sub>2</sub>O are the most prominent fluids in crustal rocks and are immiscible in the crustal P, T conditions. However, it was reported by Roedder [9], and Bodnar and Costain, [10] that the critical behavior of binary NaCl – H<sub>2</sub>O and CO<sub>2</sub> – H<sub>2</sub>O systems significantly differs from the parent H<sub>2</sub>O. Thus investigations on the mobility of these fluids in metamorphic rocks are essential in understanding metamorphic events. Famin *et al.* [3] have recently reported an elegant application of high temperature infrared microscopy for deducing qualitative information on the mobility of metamorphic fluids. They have reported a vastly different thermal evolution of the OH structure for fluid inclusions having H<sub>2</sub>O-CO<sub>2</sub>-NaCl in quartz veins and trapped under blue schist and green schist facies metamorphic conditions.

The aim of the present investigation is to extend similar studies on the fluid inclusions trapped in quartz veins emplaced in greenstone belts of the Dharwar Craton. Low grade metamorphic conditions (of upper green schist facies) prevail at the locations where gold mineralization occurs [11]. The *in-situ* infrared spectroscopy technique has been used to probe the thermal evolution of OH structure in the temperature range 25 – 300° C. Furthermore, the effect of CO<sub>2</sub> on the mobility of fluids was also investigated on the samples chosen from same metamorphic environments.

\*Address correspondence to this author at the National Geophysical Research Institute, (Council of Scientific & Industrial Research), Hyderabad – 500 606 India; Tel: 91-40-23434700; Ext: 2461; Fax: 91-40-23434651; 91-40-27171564; Email: psrprasad@ngri.res.in

## Setting

The Dharwar Craton in the Indian Peninsula (Fig. 1) is mainly made up of two groups of greenstone belts and tonalite-trondhjemite-gneisses (TTG) and separated by the NE-SW to N-S trending Closepet granites [12, 13]. The greenstone belts of the Western Dharwar Craton (WDC) were largely developed on an evolved continental crust at 3.4-2.7 Ga. The greenstone belts of the Eastern Dharwar Craton (EDC) were formed in an intra oceanic arc setting at 2.7 to 2.55 Ga ago. The grade of metamorphism of these greenstone belts largely varies between greenschist facies (core) to amphibolite facies (margins) in the different greenstone belts. The eastern margin of the Chitradurga greenstone belt in WDC, and many other greenstone belts of the EDC are traversed by transcratonic shear zones hosting gold deposits [14, 15] (Fig. 1), which are considered to be formed by epigenetic hydrothermal fluids. For example the transcratonic shear zones passing through Gadag, Hutti and Penakacherla greenstone belts host well known orogenic gold deposits/occurrences [14-16] (Fig. 1).

## MATERIALS AND METHODS

### Sample Selection

All the quartz vein samples studied were collected from different greenstone belts of the Dharwar Craton. Samples representing WDC were collected from the Hosur (BGH-5), Sangli (G1-C) and Mysore (GSM-2/6) gold mines of Gadag greenstone belt respectively, near the eastern margin of the WDC, while samples representing the EDC were collected from the Penakacherla and Hutti greenstone belts (RM5-11, RM5-16, RM5-30, RM5-33 and BT-11). One typical photo-

micrograph of the fluid inclusions studied from the Hutti gold deposit (Sample No.BT-11) is shown in Fig. (2). Details of the host rock mineralogy into which the quartz veins were emplaced and used in this study are given in Table 1. As micro-FTIR or micro-thermometry studies on the quartz vein samples were not conducted, it was not possible to characterise fluid compositions in the inclusions. However as the FTIR signatures have clearly shown the presence of H<sub>2</sub>O and CO<sub>2</sub>, the temperature-induced variations of these fluids are reported in this study.

The micro-thermometric and thermo-barometric studies carried out on the fluid inclusion bearing samples from Eastern Dharwar Craton have shown the presence of four types of fluid inclusions characterized by spatial and temporal variations [16]. Type I inclusions occur randomly within the quartz porphyroclasts; Type II inclusions occur along healed micro-fractures within the porphyroclasts; Type III inclusions are arranged along the grain boundaries while Type IV inclusions are transgranular and secondary in nature. Type I inclusions are generally of low salinity (3.9 to 13.5 wt% NaCl). All the aqueous bi-phase inclusions got homogenized in liquid state at 200 to 240 °C.

### Infrared Spectroscopy

The FTIR studies, on doubly polished slabs of 150 – 200 μm thickness, were carried out with a Thermo-Nicolet make NEXUS FTIR spectrometer (with sealed and desiccated optics) using a thermo-electrically cooled and deuterated triglycine sulfate (DTGS) detector, an extended range KBr (XT-KBr) beam splitter, and a dual source mode working in the wavenumber range of 375 - 12,500 cm<sup>-1</sup>. The spectra were recorded in the wavenumber region 2000 to 8000 cm<sup>-1</sup> using

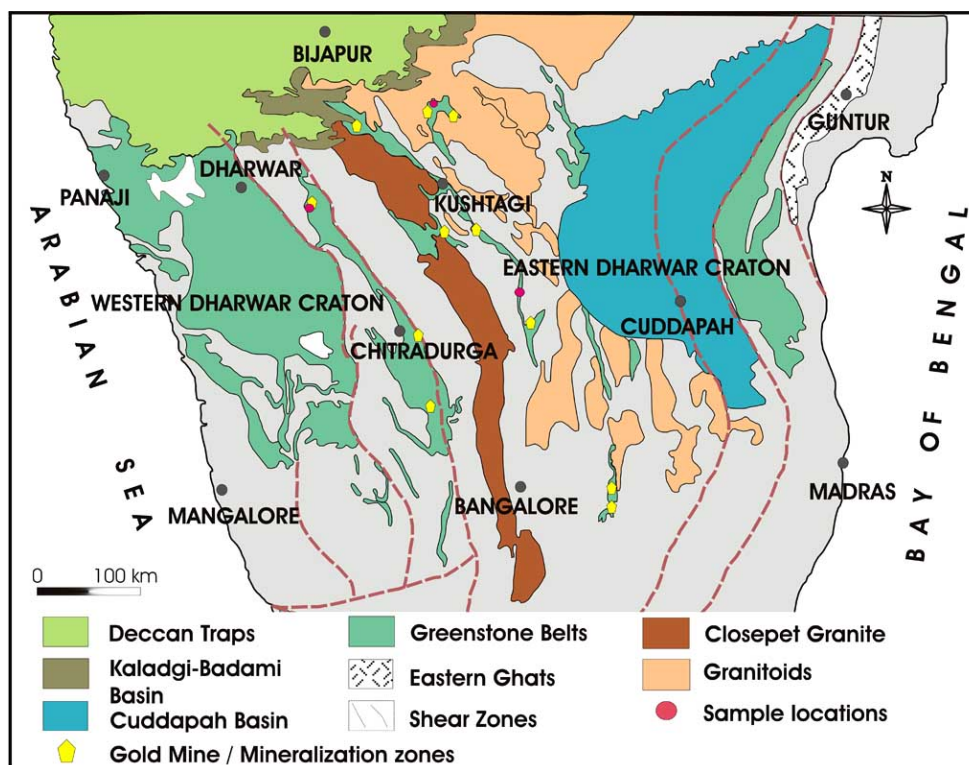
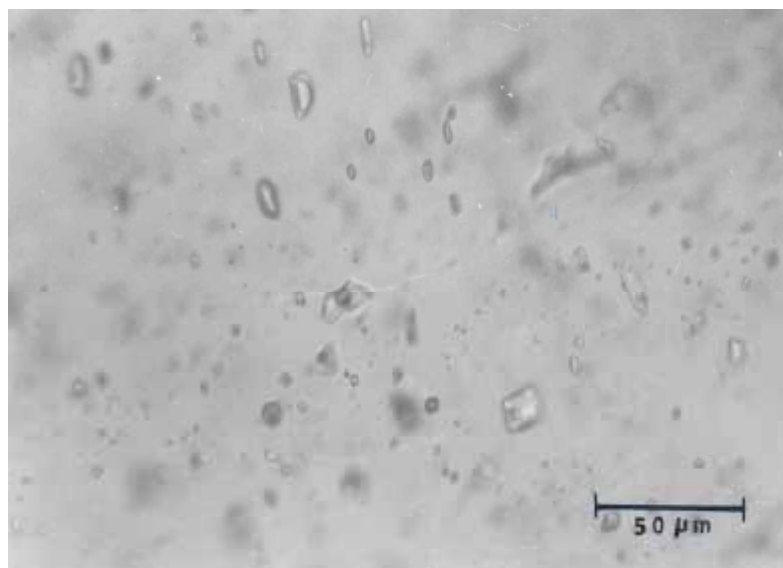


Fig. (1). Simplified geological map of the Dharwar Craton showing the distribution of greenstone belts and shear zone complexes from the Western and Eastern Dharwar Craton.



**Fig. (2).** Photomicrograph of a typical fluid inclusion within a quartz vein from the Hutti gold deposit (Sample BT-11), Eastern Dharwar Craton.

**Table 1. Details of the Samples Used in the Present Study**

Sample No.	Area	Rock Type	Mineralogy
BGH-5	Gadag Greenstone Belt, WDC Near Hosur gold mine	Meta Rhyolite	plagioclase, fine grained quartz and muscovite rich matrix $\pm$ carbonates
G-1C	Gadag Greenstone Belt, WDC Near Sangli gold mine	Meta Greywacke	Quartz, plagioclase and tiny rock fragments set in a matrix of quartz and feldspar $\pm$ carbonates
GSM- 2/6	Gadag Greenstone Belt, WDC Near Mysore gold mine	Meta basalt	Amphiboles replacing with chlorite, plagioclase. Highly carbonated
BT- 11	Hutti Greenstone Belt, EDC Hutti Gold Deposit proper	Amphibolite	Amphiboles replaced by chlorite in the ore zones, plagioclase intergrown with sericite
RM5- 11	Penakacherla Greenstone Belt, EDC Central part of the belt	Amphibolite	Hornblende, plagioclase, chlorite, epidote $\pm$ sulfides
RM5-16	Penakacherla Greenstone Belt, EDC Central part of the belt	Amphibolite	Hornblende, plagioclase, chlorite, epidote $\pm$ sulfides
RM5-30	Penakacherla Greenstone Belt, EDC Central part of the belt	Amphibolite	Hornblende, plagioclase, chlorite, epidote $\pm$ sulfides
RM5-33	Penakacherla Greenstone Belt, EDC Central part of the belt	Amphibolite	Hornblende, plagioclase, chlorite, epidote $\pm$ sulfides

a white light source (tungsten halogen) and each spectrum obtained is an average of 128 scans with a  $2\text{ cm}^{-1}$  resolution. A background spectrum was recorded at the beginning of each spectral run repeatedly using the same experimental setup, but without sample (i.e., LINKAM stage with  $\text{CaF}_2$  windows). Diameter of the aperture on the LINKAM stage was 3 mm. The accuracy in measured temperature of the LINKAM stage was carefully calibrated by measuring the surface temperature of a semi-conductor (Si wafer) by the anti-stokes and stokes Raman lines in the range -180 to 300

$^{\circ}\text{C}$  [17]. Furthermore, temperature accuracy of the LINKAM stage was checked by measuring the melting points of ice ( $0^{\circ}\text{C}$ ); tetrahydrofuran clathrate ( $4.5^{\circ}\text{C}$ ) and sulphur ( $115^{\circ}\text{C}$ ). We have recorded FTIR spectra for all the samples in the range  $-175$  to  $350^{\circ}\text{C}$  in both cooling and warming cycles at the rate of  $10^{\circ}\text{C}/\text{min}$ . The FTIR spectra at the desired temperatures were collected after about 5-8 minutes so as to attain thermal equilibrium.

Background corrected spectra were used for further analysis and the observed profiles at each temperature were

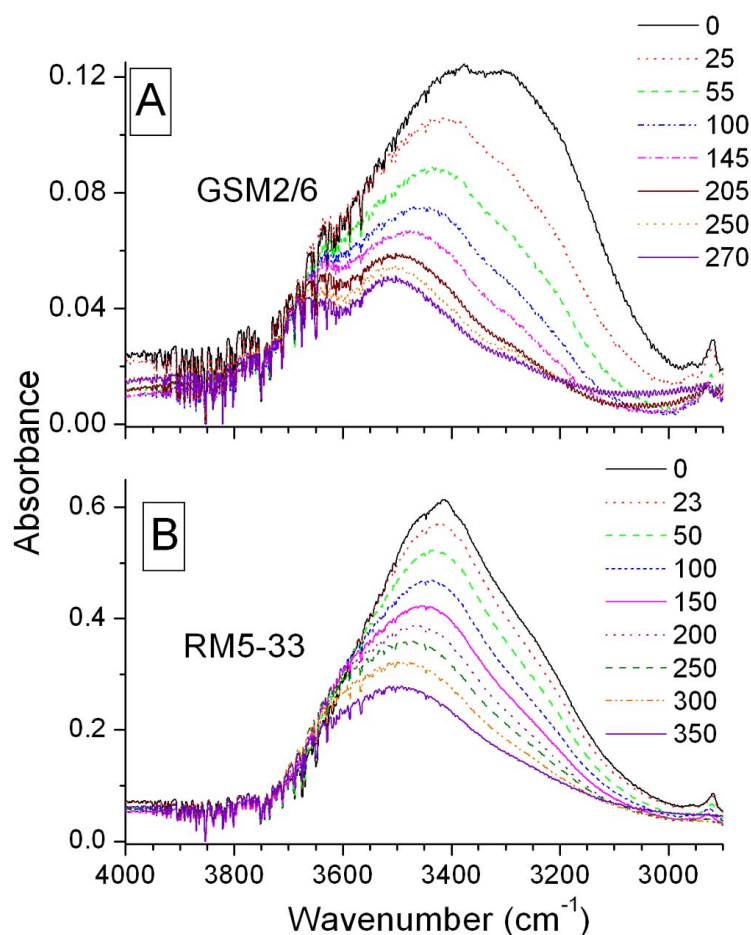


**Fig. (3).** Background corrected IR spectra of water molecules in quartz veins collected from location 1 (A) and location 4 (B) from the western and eastern parts of the Dharwar Craton, India. Corresponding temperatures are mentioned along with spectral traces. Geological locations of the analyzed samples were shown in Fig. (1).

deconvoluted into Gaussians ( $R$  is always better than 0.99) using the GRAMS/32 software and these parameters were used for further analysis. Details about the adopted procedure for deconvolution have been discussed earlier [18]. Temperature evaluation for two samples e.g., GSM-2/6 (from WDC) and RM5-33 (from EDC) is shown in Fig. (3) as a representative case. Similar spectral traces for all other samples shown in Table 1, are available upon request from the authors.

## RESULTS

All samples used in the present study have shown the infrared modes characteristic of  $H_2O$  and  $CO_2$  and therefore the fluids predominantly contain both  $H_2O$  and  $CO_2$ . The samples from the Western and Eastern parts of Dharwar Craton with comparable  $CO_2$  content (i.e., comparable absorbance ratio for  $CO_2 / H_2O$  bands) show different slopes for the OH stretching modes. Infrared spectra for water molecules were observed as a broad band centred around  $3400\text{ cm}^{-1}$ , with an additional shoulder on both the higher (due to weaker hydrogen bonding) and lower wavenumber sides (due to stronger hydrogen bonding) (Fig. 3). The sharper mode ( $\sim 3550\text{ cm}^{-1}$ ) represents the Si-OH linkage [19, 20]. The variations in the observed peak positions (deconvoluted) were plotted (systematically) for the samples from WDC &

EDC in Fig. (4). These samples were having comparable absorbance ratios for the characteristic  $CO_2$  to  $H_2O$  modes and the absorbance (due to water molecules) decreases progressively as the temperature increased from ambient. We have monitored the spectral variations during heating and cooling cycles. It was difficult to reach temperatures higher than  $275\text{ }^\circ\text{C}$  (with about 80 % decrease for water bands) in the quartz vein samples of WDC region. On the other hand a similar decrease for water bands was observed around  $350\text{ }^\circ\text{C}$  for samples of EDC.

Secondly, in order to probe the effect of  $CO_2$  on the mobility of water, we chose samples from closer locations from EDC. All the chosen samples for this study were from the central part of the Penakacherla greenstone belt of EDC (see Fig. 1), and were from similar host rock, i.e. Amphibolite, constituting the same mineralogy (Table 1). The samples were chosen within 500 meters of separation across the strike. As can be seen from (Fig. 5), a band at  $2345\text{ cm}^{-1}$  co-exists with those due to  $H_2O$ . Also the thickness of all the samples is nearly equal (evident from the nearly equal absorbance for  $SiO_2$  modes). This mode unambiguously indicates the presence of molecular  $CO_2$ . In a given thickness the total concentration of the species is proportional to the ratio of the measured absorbance to the molar absorbance ( $\epsilon^*$ ). The molar absorbance ( $\epsilon^*$ ) is grossly temperature independ-

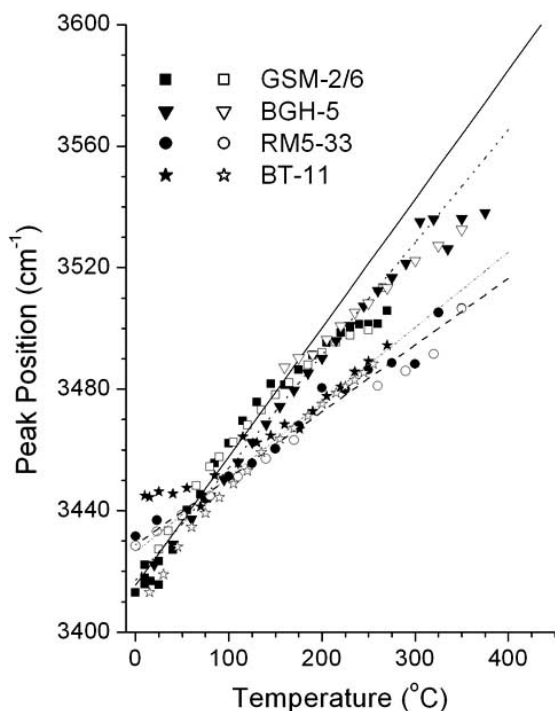


**Fig. (4).** Induced thermal variations of the peak positions of OH stretching mode in the region 0 to 350 °C. All the filled and open symbols are the peak positions during temperature increasing and decreasing cycles respectively. The lines are for the best fitted lines for the observed peak position variations.

ent and is a characteristic feature of the molecular species namely H<sub>2</sub>O; CO<sub>2</sub> or SiO<sub>2</sub> etc. Thus to a first order approxi-

mation the absorbance ratio of two bands i.e., ( $A_{CO_2} / A_{SiO_2}$ ) is proportional to their relative concentration. As can be seen from (Fig. 5), this ratio for the chosen samples varies significantly, indicating varying total CO<sub>2</sub> content. We have not observed FTIR modes characteristic of CH<sub>4</sub> etc. Further FTIR signatures of the freezing point of water molecules vary in the range of (-5° to 0° C), indicating the presence of a saline environment. On the other hand, FTIR data on warming cycle indicate that the melting of CO<sub>2</sub> does not occur at -56.6° C, showing the absence of isolated CO<sub>2</sub> inclusions. On the basis of these observations we believe that the inclusions in these quartz veins only consist of H<sub>2</sub>O and CO<sub>2</sub>. We also observed complete melting of CO<sub>2</sub> around 10 to 15 °C ( $T_{Clath}$ ) [21]. FTIR spectroscopy has previously been used to characterise clathrate formation [22]. The mobility of water inclusions were also probed in these samples by following the variations in the peak positions of OH stretching modes in the temperature range 0 to 350 °C. Observed variations were plotted in Fig. (6), in a fashion similar to Fig. (4). All the lines (continuous or broken) are the linear regressions for the experimental data. A significant variation in slope has been observed in these samples with minimum and maximum slopes at 0.22 to 0.45 cm<sup>-1</sup> °C<sup>-1</sup> for CO<sub>2</sub> poor and CO<sub>2</sub> rich samples.

**DISCUSSION**

FTIR spectrum of hydrous quartz is complicated yet carries important information about the molecular linkages in SiO<sub>2</sub> network [20]. The spectral evolution at higher temperatures could provide structurally bonded hydroxyls, water of crystallization and water inclusions. Famin *et al.* [3] have recently shown that the OH structure of metamorphic fluids of quartz veins probed by high temperature infrared spectroscopy could provide information about the trapping condi-

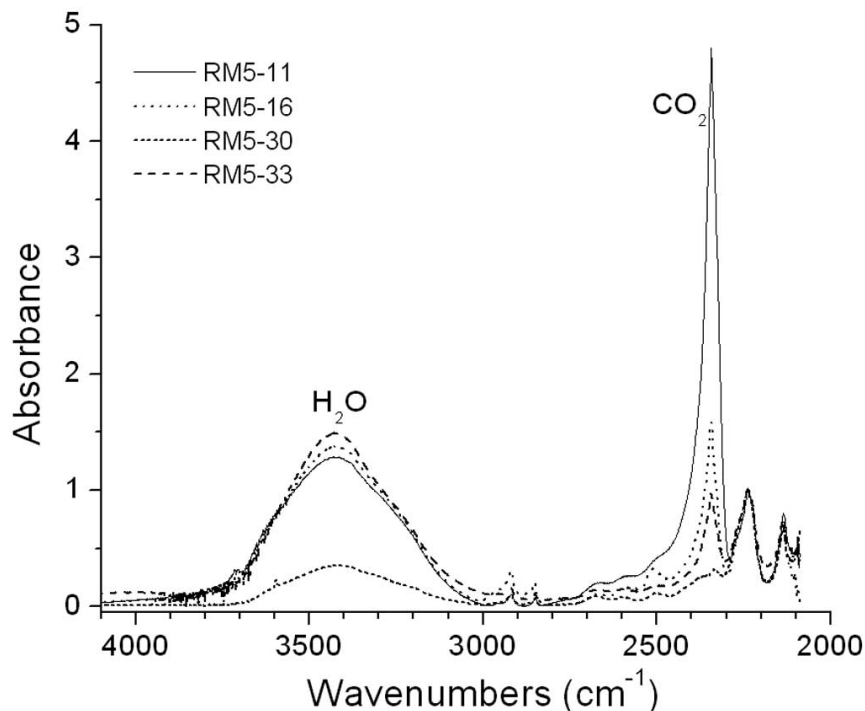


**Fig. (5).** Background corrected FTIR spectra of quartz wafers recorded at ambient temperatures (within about 500 m distance) showing varying amounts of molecular carbon dioxide.

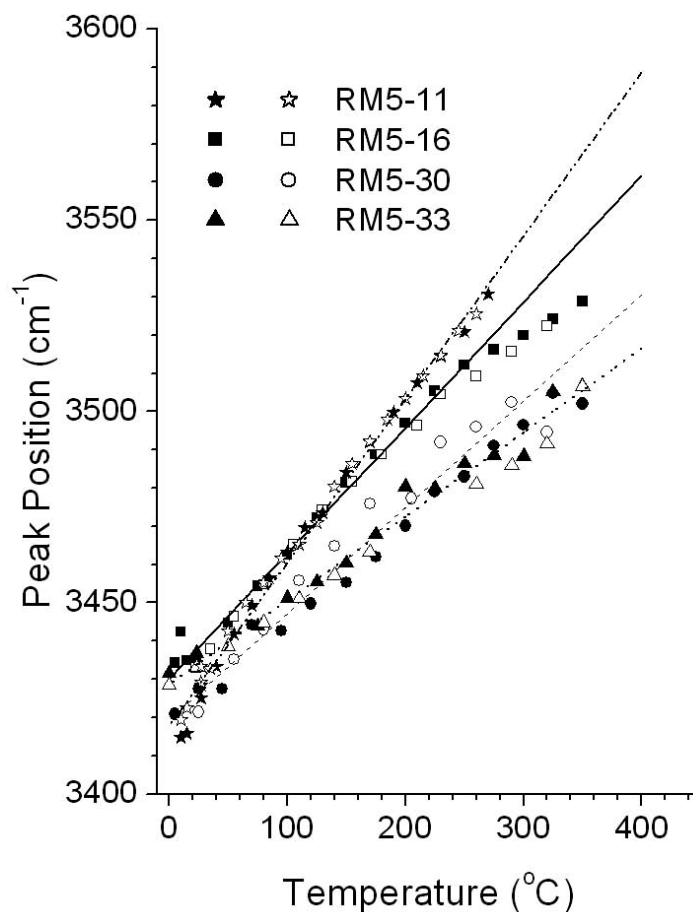


**Fig. (6).** Induced thermal variations in the peak positions of samples shown in figure 3, collected from eastern part of Dharwar Craton, in the temperature region 0 to 350 °C. All the filled and open symbols are the peak positions during temperature increasing and decreasing cycles respectively. The lines are for the best fitted lines for the observed peak position variations.

tions. The OH stretching peak position of fluids trapped under greenschist environment quasi-linearly varies at a rate of  $0.5 \text{ cm}^{-1} \text{ } ^\circ\text{C}^{-1}$  (as shown in Fig. (4)- Sample Numbers GSM-2/4, BGH-5), while the same for blueschist environment is  $0.25 \text{ cm}^{-1} \text{ } ^\circ\text{C}^{-1}$ . Extrapolated behavior at  $400^\circ \text{C}$  yielded peak positions at 3585 and  $3475 \text{ cm}^{-1}$  respectively, for greenschist and blueschist zones. In other words, the strength of hydrogen bonding for fluids trapped under greenschist metamorphic conditions is weaker and the pore structure is “loose” for fluid migration. While the behaviour for those trapped in blueschist conditions are different and the pore structure is “tight” for fluid migration. The present study is one in that direction, where we have investigated quartz veins from Dharwar Craton. Our study shows that variations of the same magnitude in the pore structures may also occur in greenschist and amphibolite facies environments.

Temperature induced variations in the peak positions of OH stretching mode for the samples of eastern part of Dharwar Craton are less comparable to those from western part (see Fig. 4). Our results indicate that the slope for the EDC is in the range  $0.22$  to  $0.28 \text{ cm}^{-1} \text{ } ^\circ\text{C}^{-1}$ , while that for WDC is in the range  $0.38$  to  $0.48 \text{ cm}^{-1} \text{ } ^\circ\text{C}^{-1}$ , with an uncertainty of  $0.1 \text{ cm}^{-1} \text{ } ^\circ\text{C}^{-1}$ . The uncertainty is mainly due to measurement errors associated with weaker and broader modes. The measurement uncertainty is still higher at elevated temperatures

and thus some points were ignored while computing the best linear fits to the observed data. Our results are comparable with those of Famin *et al.* [3]. It is also noticed that the OH stretching modes of WDC are broader and significant “leakage” of water inclusions was observed when they were subjected to heating cycle (i.e., around 40 % loss was observed between the virgin and heat treated samples). A weaker band around  $3650 \text{ cm}^{-1}$  that may be due to Si-OH bonding appears as a shoulder mode at higher temperatures [20]. All these facts are indicative of the “loose” structure of water inclusions. On the other hand the water inclusions of EDC samples are comparatively rigid and less mobile. The water loss due to “leakage” induced during the temperature cycling is around 10 %.

Our observations indicate that the fluids in these regions may have been trapped under different conditions [23]. Additionally the FTIR spectrum of molecular  $\text{CO}_2$  region (Fig. 7) at  $-60^\circ \text{C}$  is vastly different for both EDC and WDC samples. The band around  $2443 \text{ cm}^{-1}$  in both the samples shifts to lower wave number by  $8 \text{ cm}^{-1}$  indicating solid  $\text{CO}_2$  phase at  $-60^\circ \text{C}$  [21]. However, an additional mode around  $2273 \text{ cm}^{-1}$  is clearly seen in all the samples from EDC indicating the presence of  $^{13}\text{C}$ . We did not observe this mode in WDC samples even at lower temperatures ( $-175^\circ \text{C}$ ). Thus, we conclude that the fluids of EDC and WDC might have been

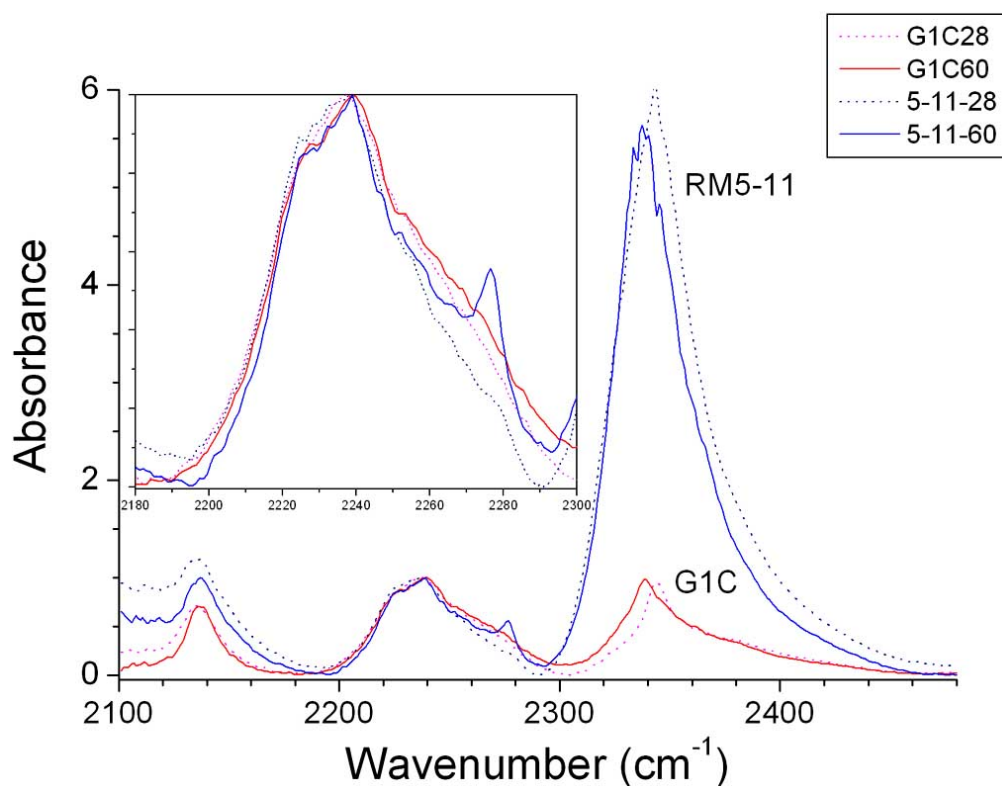


**Fig. (7).** The FTIR spectrum of molecular CO<sub>2</sub> in quartz veins of EDC and WDC at 27 (dotted line) and –60 °C (solid line). Inset shows the (<sup>13</sup>C-O) asymmetric stretching mode at 2274 cm<sup>-1</sup> in EDC in expanded scale.

trapped under different metamorphic environments and the source for carbonic inclusions of EDC may have been deeper when compared to WDC.

It has been shown that the pore textures equilibrated with Na<sup>+</sup>- K<sup>+</sup>- Mg<sup>2+</sup>- Ca<sup>2+</sup>- Cl<sup>-</sup> rich fluids have lower dihedral angles and lower solid-fluid interfacial energies, while those equilibrated with CO<sub>2</sub> – containing fluids display higher dihedral angles. In other words the salinity ‘softens’ the fluid flow, while CO<sub>2</sub> ‘hardens’ and the fluids remains in a “closed” environment. This concept was used by Famin *et al.* [3] in immiscible CO<sub>2</sub> – H<sub>2</sub>O inclusions and reported increasing mobility for H<sub>2</sub>O in samples without and with (trace) CO<sub>2</sub> from greenschist facies (sample III and IIIa in their study) of Tinos Island, Greece. However, this cannot be applicable in the present study as CO<sub>2</sub> – H<sub>2</sub>O fluids exist in a bi-phase mode. In the case of mixed phase inclusions trapped in calcite, it was observed that the dihedral angle decreases from 80° to 50° in 0.0 < X<sub>CO2</sub> < 0.5 and increases at higher CO<sub>2</sub> concentrations and the exact reason for the well defined minima at X<sub>CO2</sub> = 0.5 was not understood [24, 25]. However no such minima were reported for quartz-fluid dihedral angle and it showed a monotonous increase with increasing CO<sub>2</sub> content. As can be seen in Fig. (6), we probed the fluid migration in four samples with significantly different (CO<sub>2</sub>/SiO<sub>2</sub>) ratios. As already explained this ratio could be used as a measure of CO<sub>2</sub> contents. The peak positions of OH stretching mode vary linearly with slopes 0.28; 0.24; 0.33 and 0.43 cm<sup>-1</sup> °C<sup>-1</sup> for samples in which (CO<sub>2</sub>/SiO<sub>2</sub>) ratio respectively is trace (RM5-33); 0.3 (RM5-30); 1.06 (RM5-16) and 4.21 (RM5-11). It is difficult to attribute the cause for such an increase and more experimental work is

necessary on a wide number of samples. However, appearance of <sup>13</sup>C related signals (Fig. 7) and higher mobility for CO<sub>2</sub> rich samples of EDC clearly demarcate that the origin of metamorphic fluids in these regions are different. Generally the mobility of fluids was showing an increasing trend with an increase in CO<sub>2</sub> content under similar metamorphic conditions.

## CONCLUSIONS:

In summary we studied temperature dependent behavior of the fluid inclusions in quartz veins from different locations of Dharwar Craton, India using in-situ FTIR spectroscopy in the range 0 to 350 °C.

The samples of western Dharwar Craton have shown higher slopes of water band variation with temperatures (0.37 to 0.46 cm<sup>-1</sup> °C<sup>-1</sup>), suggesting a higher mobility of metamorphic fluids. On the other hand, the samples from eastern part vary in the range (0.22 to 0.25 cm<sup>-1</sup> °C<sup>-1</sup>), suggesting a lower mobility of fluids trapped in these samples. Nearly 40 % of water loss was observed in the samples of WDC, whereas it was smaller in samples of EDC indicating that the pore texture and entrapment conditions may be different. This fact was corroborated by the observation of (<sup>13</sup>C-O) asymmetric stretching mode at 2274 cm<sup>-1</sup> in EDC samples at sub-ambient temperatures.

The effect of multi- phase fluids (CO<sub>2</sub> – H<sub>2</sub>O – NaCl) on the mobility was also probed in some closely separated quartz vein samples from EDC. Mobility was observed to increase with CO<sub>2</sub> and the slopes vary in the range (0.22 to 0.43 cm<sup>-1</sup> °C<sup>-1</sup>).

## ACKNOWLEDGEMENTS

Authors sincerely thank the Director, National Geophysical Research Institute, Hyderabad, for his encouragement, and permission to publish this paper. Research grant from the Department of Science and Technology (DST) to PSRP is gratefully acknowledged.

## REFERENCES

- [1] Fyfe, W.S.; Price, N.J.; Thompson, A.B. Fluids in the earth's crust.; Elsevier: Amsterdam, **1978**.
- [2] Famin, V.; Nakashima, S. Fluid migration in fault zones and the evolution of detachments: The example of Tinos Island (Greece) in Phisicochemistry of Water in Geological and Biological Systems; Nakashima, S.; Spiers, C.J.; Mercury, L.; Fenter, P.A.; and Hochella, M.F. Jr., Eds.; Universal Academy Press INC: Tokyo, Japan, **2004**.
- [3] Famin, V.; Nakashima, S.; Jolivet, L.; Philippot, P. Mobility of metamorphic fluids inferred from infrared microspectroscopy on natural fluid inclusions: the example of Tinos Island, Greece. *Contrib. Mineral. Petrol.*, **2004**, *146*, 736-49.
- [4] Hiraga, T.; Nishikawa, O.; Nagase, T.; Akizuki, M. Morphology of intergranular pores and wetting angles in pelitic schists studied by transmission electron microscopy. *Contrib. Mineral. Petrol.*, **2001**, *141*, 613-622.
- [5] Morrison, J.; Anderson, J.L. Footwall refrigeration along a detachment fault: implications for the thermal evolution of core complexes. *Science*, **1998**, *279*, 63-66.
- [6] Watson, E.B.; Brenan, J.M. Fluids in the lithosphere, 1: experimentally-determined wetting characteristics of CO<sub>2</sub>-H<sub>2</sub>O fluids and their implications for fluid transport, host-rock physical properties, and fluid inclusion formation. *Earth Plant. Sci. Lett.*, **1987**, *85*, 497-515.
- [7] Holness, M.B. Equilibrium dihedral angles in the system quartz-CO<sub>2</sub>-H<sub>2</sub>O-NaCl at 800°C and 1-15 kbar: the effects of pressure and fluid composition on the permeability of quartzites. *Earth Plant. Sci. Lett.*, **1992**, *114*, 171-184.
- [8] Holness, M.B. Temperature and pressure dependence of quartz aqueous fluid dihedral angles: the control of adsorbed H<sub>2</sub>O on the permeability of quartzites. *Earth Plant Sci. Lett.*, **1993**, *117*, 363-377.
- [9] Roedder, E. Fluid Inclusion Evidence Bearing on the Environments of Gold Deposition. In: *Gold '82 I*, Foster, R.P., Ed.; Geological Society of Zimbabwe, Special Publication **1984**; pp. 129-163.
- [10] Bodnar, R.J.; Costain, J.K. Effect of varying fluid composition on mass and energy-transport in the earth's crust, *Geophys. Res. Lett.*, **1991**, *18*, 983-986.
- [11] Ugarkar, A.G. Implications of retrograde metamorphism for gold mineralisation in the greenstone belts of Northern Dharwar Craton, Karnataka, India. *Gond Res.*, **1998**, *1*, 215-219.
- [12] Radhakrishna, B.P. *The Closepet Granite of Mysore state*. Mysore Geological Association (Bangalore) Special Publication, India **1956**, vol. 3.
- [13] Naqvi, S.M.; Rogers, J.J.W. *Precambrian Geology of India, Oxford Monographs on Geology and Geophysics No.6*, Oxford University Press: New York, **1987**.
- [14] Manikyamba, C.; Naqvi, S.M.; Ram Mohan, M; Gnaneshwar Rao, T. Gold mineralisation and alteration of Penakacherla Schist Belt, India: Constraints on Archaean subduction and fluid processes. *Ore Geol. Rev.* **2004**, *24*, 199-227.
- [15] Kolb, J.; Rogers, A.; Meyer, F.M. Relative timing of deformation and two-stage gold mineralization at the Hutti Mine, Dharwar Craton, India. *Mineral Deposita*, **2005**, *40*, 156-174.
- [16] Pal, N.; Mishra, B. Alteration geochemistry and fluid inclusion characteristics of the greenstone hosted gold deposit of Hutti, Eastern Dharwar Craton, India. *Mineral Deposita*, **2002**, *37*, 722-736.
- [17] Prasad, P.S.R. Micro-Raman spectroscopy for measuring surface temperature of semiconductor. *J Nondestruct Eval.* **2009** (in press).
- [18] Prasad, P.S.R.; Chaitanya, V.K.; Prasad, K.S.; Rao, D.N. Direct formation of  $\gamma$ -CaSO<sub>4</sub> phase in dehydration process of gypsum: *In-situ* FTIR study. *Am. Mineral.*, **2005**, *90*, 672-678.
- [19] Masuda, K.; Haramaki, T.; Nakashima, S.; Martinez, I.; Kashiwbara, S. Structural changes of water with solutes and temperature up to 100°C in aqueous solutions as revealed by ATR-IR spectroscopy. *Appl. Spectrosc.* **2003**, *57*, 274-281.
- [20] Ram Mohan, M.; Prasad, P.S.R. FTIR investigations on the fluid inclusions in quartz veins of the Penakacherla schist belt. *Curr. Sci.* **2002**, *83*, 755-760.
- [21] Prasad, P.S.R.; Shiva Prasad, K.; Thakur, N.K. FTIR signatures of type-II clathrates of carbon dioxide in natural quartz veins. *Curr. Sci.* **2006**, *90*, 1544-1547.
- [22] Fleyfel, F.I.; Devlin, J.P. Carbon dioxide clathrate hydrate epitaxial growth: Spectroscopic evidence for formation of the simple type-II CO<sub>2</sub> hydrate. *J Phys. Chem.*, **1991**, *95*, 3811-3815.
- [23] Naqvi, S.M. *Geology and Evolution of the Indian Plate (From Hadean to Holocene – 4 Ga to 4 Ka)*. Capital Publishing Company: New Delhi, **2005**.
- [24] Holness, M.B.; Graham, C.M. Equilibrium dihedral angles in the system H<sub>2</sub>O-CO<sub>2</sub>-NaCl-calcite, and implications for fluid flow during metamorphism. *Contrib. Mineral. Petrol.*, **1991**, *108*, 368-383.
- [25] Holness, M.B.; Graham, C.M. P-T-X effect on equilibrium carbonate-H<sub>2</sub>O-CO<sub>2</sub>-NaCl dihedral angles: constraints on carbonate permeability and the role deformation during metamorphism. *Contrib. Mineral. Petrol.*, **1995**, *119*, 301-313.

Received: May 05, 2009

Revised: November 17, 2009

Accepted: November 25, 2009

© Sarma et al.; Licensee Bentham Open.

This is an open access article licensed under the terms of the Creative Commons Attribution Non-Commercial License (<http://creativecommons.org/licenses/by-nc/3.0/>) which permits unrestricted, non-commercial use, distribution and reproduction in any medium, provided the work is properly cited.